

# Joint Blind Timing Synchronization and Channel Estimation for OFDM using Receiver Diversity

Qi Cheng, Hao Wang and Biao Chen

Syracuse University, Department of EECS, 121 Link Hall, Syracuse, NY 13244

## Abstract

Joint blind timing synchronization and channel estimation using receiver diversity are investigated in this paper. If the channel length is smaller than the cyclic prefix length, the diversity based timing synchronization can achieve perfect timing estimator at high SNR. At low SNR, multiple blocks can be used to improve the performance. The proposed algorithm is able to identify channel length, therefore it can facilitate blind channel estimation algorithms that require the knowledge of channel length.

## 1 Introduction

Orthogonal frequency division multiplexing (OFDM) systems have recently gained increased interest due to its high data rate transmission capability with high bandwidth efficiency and its robustness to multipath delay spread. However, as a multicarrier transmission scheme, it is also very sensitive to timing and frequency synchronization error. To assure no (or low) inter-carrier interference (ICI) and inter block interference (IBI), OFDM receiver has to identify the symbol boundaries and the optimal timing instances. In [1][2], training symbol based timing synchronization was proposed where a symbol with two identical halves in time domain is used for synchronization. In [3], the authors proposed a method of joint timing and channel estimation by using training symbols as specified in wireless LAN standard, which is stemmed from that of [1]. While these training symbol based synchronization schemes are resource consuming, their performance is also limited for the following reasons. Training symbols are usually embedded in between payload bursts that are usually of much longer duration for bandwidth efficiency. Thus the synchronization is usually limited to the use of only one training symbol (or block) in delay sensitive applications. The inability of utilizing multiple training symbols limits the performance of these methods. Blind symbol timing synchronization, on the other hand, has the advantages of higher bandwidth efficiency as it does not require the transmission of training symbols. Further, consecutive blocks can be used jointly to improve the

performance without imposing significant delay. In [4], a blind synchronization algorithm is proposed where the correlation of cyclic prefix with its corresponding part at the end of the OFDM symbol block is used. The method, however, is developed based on the additive white Gaussian noise (AWGN) channel assumption and will suffer error floor effect in the presence of time-dispersive channel at large SNR.

Separately in [5], a blind channel estimation using receiver diversity for coherent OFDM detection was proposed. The algorithm, however, requires the perfect knowledge of the exact timing instance and the channel length. In this paper, we propose an algorithm of joint blind timing and channel estimation for OFDM by exploiting channel diversity. The paper is organized as follows. In Section 2, the problem under consideration is formulated. Then we briefly present the blind channel estimation algorithm of [5]. In Section 3, we provide the algorithm for joint timing and channel estimation without knowing the channel length. Numerical examples are given in Section 4. Finally, we conclude the paper in Section 5.

## 2 Statement of the problem

The basic principles of the OFDM technique have been described in detail in [6]. The transmitter and receiver block diagrams of an OFDM system are shown in Fig. 1, where the modulation and demodulation processes are efficiently implemented through the fast Fourier transform (FFT) algorithm.

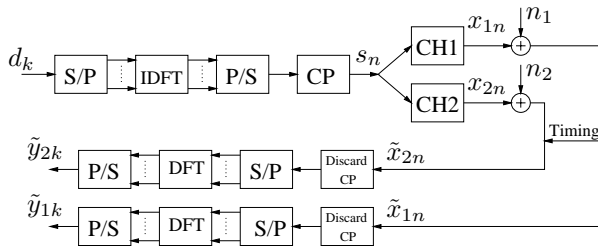


Figure 1: Block diagram of an OFDM system using receiver diversity

In OFDM systems,  $N$  subcarriers are used to mod-

ulate information symbols to construct one OFDM symbol. Cyclically extended guard time is inserted to maintain inter-carrier orthogonality in the presence of time-dispersive channel [6]. We consider frequency-selective fading channels by modeling the channel impulse response as a finite impulse response (FIR) filter with the filter length assumed to be shorter than the cyclic prefix length. Because the algorithm provided in this paper is based on the receiver diversity, two receivers are used in the diagram. These two receivers can be realized either through the use of two receive antennas or via oversampling. For the oversampling approach, it is easy to achieve synchronization between the two channels.

In [5], we assume that the exact timing instance  $CP + 1$  ( $CP$  is the length of cyclic prefix) and the channel length  $L$  are known. The received signals, after carrier frequency synchronization and application of DFT, can be written as <sup>1</sup>

$$\begin{aligned}\tilde{\mathbf{y}}_1 &= \mathbf{H}_1 \mathbf{d} + \mathbf{z}_1 \\ \tilde{\mathbf{y}}_2 &= \mathbf{H}_2 \mathbf{d} + \mathbf{z}_2\end{aligned}\quad (1)$$

where  $\mathbf{H}_i = \text{diag}(\mathbf{h}_i)$  with  $\mathbf{h}_i = [H_i(0), \dots, H_i(N-1)]^T$ ,  $H_i(k)$  is the channel frequency response corresponding to the  $i$ th channel at subcarrier  $k$ ,  $\mathbf{d} = [d_0, \dots, d_{N-1}]^T$  is the symbol vector, and  $\mathbf{z}_1$  and  $\mathbf{z}_2$  are additive white complex Gaussian noise and are uncorrelated with each other. Using simple matrix algebra, we can rewrite the signal model as

$$\begin{aligned}\tilde{\mathbf{y}}_1 &= \mathbf{D} \mathbf{h}_1 + \mathbf{z}_1 = \mathbf{D} \mathbf{W}_L \mathbf{g}_1 + \mathbf{z}_1 \\ \tilde{\mathbf{y}}_2 &= \mathbf{D} \mathbf{h}_2 + \mathbf{z}_2 = \mathbf{D} \mathbf{W}_L \mathbf{g}_2 + \mathbf{z}_2\end{aligned}\quad (2)$$

where  $\mathbf{D} = \text{diag}(\mathbf{d})$  and  $\mathbf{g}_i$  is the impulse response for the  $i$ th channel and is of length  $L$ .  $\mathbf{W}_L$  is the first  $L$  columns of the DFT matrix  $\mathbf{W}$ . Further we can write  $\mathbf{W}_L = [\mathbf{u}_1, \dots, \mathbf{u}_N]^H$  where each  $\mathbf{u}_k$  is an  $L$  by 1 vector.

Let  $\mathbf{y}_i (i = 1, 2)$  denote the noiseless received signal, then we have

$$\mathbf{y}_i = \mathbf{H}_i \mathbf{d} = \mathbf{D} \mathbf{W}_L \mathbf{g}_i \quad (3)$$

and

$$\tilde{\mathbf{y}}_i = \mathbf{y}_i + \mathbf{z}_i \quad (4)$$

In the noiseless case, using element-by-element cross multiplication, it is easy to show that

$$y_1(k) \mathbf{u}_k^H \mathbf{g}_2 = y_2(k) \mathbf{u}_k^H \mathbf{g}_1 \quad (5)$$

The matrix form of the above equation is

$$\mathbf{Y}_1 \mathbf{W}_L \mathbf{g}_2 = \mathbf{Y}_2 \mathbf{W}_L \mathbf{g}_1 \quad (6)$$

<sup>1</sup>Throughout the paper, we use bold face capital letters to denote matrices while bold face small letters to denote vectors.

where  $\mathbf{Y}_i = \text{diag}(\mathbf{y}_i)$ ,  $i = 1, 2$ . Equivalently, we have

$$\begin{bmatrix} \mathbf{Y}_2 \mathbf{W}_L & -\mathbf{Y}_1 \mathbf{W}_L \end{bmatrix} \begin{bmatrix} \mathbf{g}_1 \\ \mathbf{g}_2 \end{bmatrix} = 0 \quad (7)$$

Therefore, the channel can be retrieved up to a scalar ambiguity by simply finding a solution for the above homogeneous equation. The equation can be expressed in a quadratic form:  $\mathbf{g}^H \mathbf{V}^H \mathbf{V} \mathbf{g} = 0$  where  $\mathbf{g} = [\mathbf{g}_1, \mathbf{g}_2]^T$  and  $\mathbf{V} = [\mathbf{Y}_2 \mathbf{W}_L \quad -\mathbf{Y}_1 \mathbf{W}_L]$ . This allows the easy extension to the noisy case. Define  $\tilde{\mathbf{V}} = [\tilde{\mathbf{Y}}_2 \mathbf{W}_L \quad -\tilde{\mathbf{Y}}_1 \mathbf{W}_L]$ . Instead of finding the exact solution we simply try to minimize the quadratic term  $\tilde{\mathbf{V}}^H \tilde{\mathbf{V}}$  under a unit norm constraint. The solution is the eigenvector corresponding to the smallest eigenvalue of the matrix  $\tilde{\mathbf{V}}^H \tilde{\mathbf{V}}$ , which is equivalent to finding the right singular vector corresponding to the smallest singular value of  $\tilde{\mathbf{V}}$ .

If the channel response is quasi-stationary when we can assume that it remains constant during several OFDM blocks, channel estimation can be improved by utilizing multiple OFDM blocks. Assume  $K$  blocks are used for channel estimation. It is straightforward to extend the algorithm to the following minimization problem:

$$\min_{\mathbf{g}} \mathbf{g}^H \left[ \sum_{k=1}^K \tilde{\mathbf{V}}_k^H \tilde{\mathbf{V}}_k \right] \mathbf{g} \quad \text{s.t. } |\mathbf{g}| = 1 \quad (8)$$

where  $\tilde{\mathbf{V}}_k$  is constructed for each OFDM block.

The above channel estimation algorithm is based on the exact knowledge of the timing and the channel length. In the next section, the joint blind timing and channel length estimation algorithm by exploiting receiver diversity is provided.

### 3 Joint timing and channel estimation

It is known that the symbol timing  $q$  may vary over an interval  $[L, CP + 1]$  without causing ICI or IBI if the channels are assumed to be of shorter length than that of the cyclic prefix, i.e.  $L \leq CP$ . In this case, the orthogonality between the subcarriers won't be destroyed. It only introduces a different phase shift for each subcarrier,

$$\phi_k = 2\pi f_k \tau \quad k = 0, 1, \dots, N-1$$

where  $\tau$  is the timing offset defined as  $CP + 1 - q$ . Suppose  $\bar{\mathbf{g}}_i$  is the channel impulse response of length  $CP$  with zeros appended to  $\mathbf{g}_i$  for  $i = 1, 2$ , and  $\mathbf{W}_{CP}$  is the matrix composed of the first  $CP$  columns of the DFT matrix  $\mathbf{W}$  and  $\mathbf{W}_{CP} = [\bar{\mathbf{u}}_1, \dots, \bar{\mathbf{u}}_N]^H$ , where each  $\bar{\mathbf{u}}_k$  is now a  $CP$  by 1 vector. In the noiseless case, we have

$$y_i(k) = d_{(k-\tau)} \bar{\mathbf{u}}_{(k-\tau)}^H \bar{\mathbf{g}}_i \quad (9)$$

Here,

$$(k - \tau) = \begin{cases} k - \tau & \text{if } k \geq \tau \\ k - \tau + N & \text{if } k < \tau \end{cases}$$

By cross multiplication, we have

$$y_1(k) \bar{\mathbf{u}}_{(k-\tau)}^H \bar{\mathbf{g}}_2 = y_2(k) \bar{\mathbf{u}}_{(k-\tau)}^H \bar{\mathbf{g}}_1 \quad (10)$$

By defining rotation matrix

$$\mathbf{R} = \text{diag}([1, e^{-j2\pi \frac{\tau}{N}}, e^{-j2\pi \frac{2\tau}{N}}, \dots, e^{-j2\pi \frac{(N-1)\tau}{N}}]),$$

the matrix form of equation (10) can be written as

$$\mathbf{Y}_1 \mathbf{W}_{CP} \mathbf{R} \bar{\mathbf{g}}_2 = \mathbf{Y}_2 \mathbf{W}_{CP} \mathbf{R} \bar{\mathbf{g}}_1 \quad (11)$$

Equivalently,

$$\begin{bmatrix} \mathbf{Y}_2 \mathbf{W}_{CP} & -\mathbf{Y}_1 \mathbf{W}_{CP} \end{bmatrix} \begin{bmatrix} \mathbf{R} & \mathbf{0} \\ \mathbf{0} & \mathbf{R} \end{bmatrix} \begin{bmatrix} \bar{\mathbf{g}}_1 \\ \bar{\mathbf{g}}_2 \end{bmatrix} = \bar{\mathbf{V}} \mathbf{g}' = 0 \quad (12)$$

**Lemma 1** *If the timing instance  $q$  satisfies  $L \leq q \leq CP + 1$ , there exists  $\mathbf{g}^*$  such that*

$$\bar{\mathbf{V}}(q) \mathbf{g}^* = 0 \quad (13)$$

Equation (13) also implies  $\min \text{eig}(\bar{\mathbf{V}}(q)^H \bar{\mathbf{V}}(q)) = 0$  for those timing instances  $q$ . If the timing offset  $\tau$  is 0, we have  $\mathbf{g}^* = \bar{\mathbf{g}}$  up to a scalar constant [5]. Otherwise we have  $\mathbf{g}^* = \mathbf{R} \bar{\mathbf{g}}$  and this results in a phase rotation of the output. If the timing offset  $\tau$  exceeds the region,  $\bar{\mathbf{V}}(q)^H \bar{\mathbf{V}}(q)$  is full rank and  $\min \text{eig}(\bar{\mathbf{V}}(q)^H \bar{\mathbf{V}}(q))$  is going to be much larger. Fig. 2 is an example of

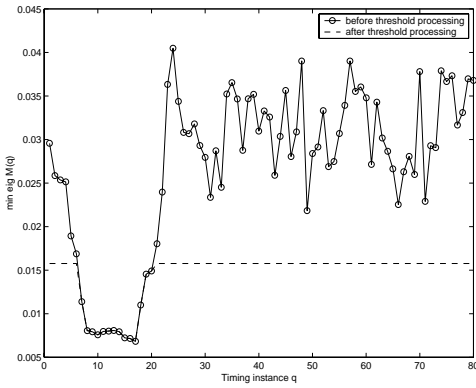


Figure 2: Example of the output statistic for timing synchronization. The true ICI/IBI-free timing interval is between 8 and 17 (inclusive).

the minimum eigenvalue of  $\bar{\mathbf{V}}^H \bar{\mathbf{V}}$  as a function of the timing instance. We notice that there is always a flat

bottom region corresponding to the ICI/IBI-free instances.

At the first stage of the timing synchronization, those instances should be identified. We also need to know the exact block timing instance (or initial phase) to avoid (or to be able to correct) possible phase rotation of the demodulated symbols. This can be achieved by recognizing that the last point of the ICI/IBI-free region, i.e.,  $CP + 1$ , corresponds to the “perfect timing” instance in a sense that it will not introduce any phase rotation if it is the starting point of DFT. In the noiseless case, the ICI/IBI-free instances start from  $L$  to  $CP + 1$ , so by identifying this region which is of length  $CP - L + 2$ , we can estimate the channel length that can be used for blind channel estimation.

### 3.1 Preprocessing in Identification of the ICI/IBI-free timing instances

The identification of ICI/IBI-free timing region is not a trivial task. Because of noise, the minimum eigenvalue of matrix  $\bar{\mathbf{V}}^H \bar{\mathbf{V}}$  deviates from 0.

To facilitate timing synchronization based on the  $\mathbf{V}$  matrix, we first study the minimum eigenvalues  $M(q)$  as a function of timing instance  $q$ :

$$M(q) = \min \left[ \text{eig}(\bar{\mathbf{V}}(q)^H \bar{\mathbf{V}}(q)) \right] \quad (14)$$

**Theorem 1** *If the timing instance  $q$  satisfies*

$$L \leq q \leq CP + 1$$

*we have*

$$\text{E}(\bar{\mathbf{V}}^H \bar{\mathbf{V}}) = \bar{\mathbf{V}}^H \bar{\mathbf{V}} + \sigma^2 \mathbf{I} \quad (15)$$

*and*

$$\min \left[ \text{eig}(\text{E}(\bar{\mathbf{V}}^H \bar{\mathbf{V}})) \right] = \sigma^2 \quad (16)$$

*where  $\sigma^2$  is the noise power and  $\mathbf{I}$  is identity matrix with the same dimension of matrix  $\bar{\mathbf{V}}^H \bar{\mathbf{V}}$ .*

If the timing instance  $q$  is out of the interval, even though  $M(q)$  is also increased by  $\sigma^2$  on the average, it is much larger than that for ICI/IBI-free region due to the fact that  $\bar{\mathbf{V}}^H \bar{\mathbf{V}}$  is full rank. When plotting  $M(q)$  as a function of the timing instance  $q$ , we always have a shape of upside down trapezoid correspondingly.

Since we are only interested in the upside down trapezoid part, we can first preprocess the output to eliminate the effect from non ICI/IBI-free region. A heuristic way is to set a threshold. Since the value of  $M(q)$  is a function of noise power, the threshold is not a constant, but SNR dependent. In practice, SNR is not known *a priori*. Therefore, we choose the threshold based on the available data  $M(q)$ . Let  $M_{max} =$

$\max(M(q)), M_{min} = \min(M(q))$ . The threshold is chosen as

$$Th = M_{min} + (M_{max} - M_{min})/3 \quad (17)$$

and set

$$M(q) = \begin{cases} Th & \text{if } M(q) > Th \\ M(q) & \text{if } M(q) \leq Th \end{cases} \quad (18)$$

The number 3 in the formular for the threshold was chosen empirically after it was found to provide accurate simulation results.

This is a preprocessing step and the purpose is to roughly refine the region of interest and eliminate the impact from non ICI/IBI- free region. The experiments show that this heuristic approach works well for a large range of SNR ( $SNR \geq 10\text{dB}$ ).

### 3.2 Multiphase Linear Regression

In Fig. 2, we can see clearly that after the preprocessing, the region of ICI/IBI-free timing instances is much easier to identify than directly from original data. The bottom of the upside down trapezoid is exactly the region we are looking for. Its last point is the “perfect timing instance” without introducing any phase rotation; and its length is equal to  $CP - L + 2$ . This trapezoid, however, is not perfect in the sense that its edges have jitteries due to the noise in the observation. Since the trapezoid can be approximated by three lines, multiphase linear regression analysis [7] is used here to model this shape:

$$M(q) = \begin{cases} \beta_{10} + \beta_{11}q & q_0 \leq q \leq sp \\ \beta_{20} + \beta_{21}q & sp \leq q \leq ep \\ \beta_{30} + \beta_{31}q & ep \leq q \leq q_1 \end{cases} \quad (19)$$

where  $sp$  and  $ep$  are start-point and end-point of the bottom line respectively.  $[q_0, q_1]$  is the region refined after the preprocessing by the threshold. In Fig. 2, we have  $q_0 = 5, q_1 = 20$  and  $sp = 8, ep = 17$ . Our least square estimation of the ICI/IBI- free region is

$$\min_{\hat{sp}, \hat{ep}, \beta} (M(\mathbf{q}) - \hat{M}(\mathbf{q}))^2 \quad (20)$$

where

$\mathbf{q} = [q_0, \dots, q_1]^T$  and  $\beta = [\beta_{10}, \beta_{11}; \beta_{20}, \beta_{21}; \beta_{30}, \beta_{31}]$ . The corresponding estimate of the timing instance is

$$\hat{q} = \hat{ep} \quad (21)$$

and the estimate of the channel length

$$\hat{L} = CP + 2 - (\hat{ep} - \hat{sp} + 1) \quad (22)$$

Once we have the start timing instance and the channel length, the algorithm provided in section 2 can be used to estimate the channel and retrieve the input symbols.

## 4 Numerical Examples

In this section, several Monte Carlo simulation results are provided to illustrate the effectiveness of our algorithm. In all simulations, we consider an OFDM system with 64 subcarriers and cyclic prefix of length  $CP = 16$ . Randomly generated QPSK symbols are used as input symbols. The following channel pair is generated randomly as Rayleigh fading channels with unit norm and channel length  $L = 8$ :

$$\begin{aligned} \mathbf{g}_1 &= [.12 + .06i, -.13 + .06i, .1 - .15i, .19 - .12i, \\ &\quad -.25 + .08i, .23 - .17i, .03 + .31i, .78 - .15i]^T \\ \mathbf{g}_2 &= [-.15 - .12i, .19 - .06i, .11 + .19i, -.13 + .18i, \\ &\quad .04 - .28i, -.22 + .26i, .5 - .14i, -.59 + .07i]^T \end{aligned}$$

The channels are fixed during the multiple OFDM blocks used to improve the performance. This is reasonable given the quasi-stationary channel response assumption.

- **Timing estimation** The mean value of timing estimation is very close to the true value 17. The mean-squared error of timing estimation is provided in Fig. 3. For  $SNR > 20\text{dB}$ , the MSE is less than  $10^{-3}$  based on 1000 Monte Carlo runs and we can always achieve perfect timing estimation.
- **Estimation of the effective channel length** The mean value of channel length estimation is very close to the true value 8. The mean-squared error of channel length estimation is provided in Fig. 4. For  $SNR > 20\text{dB}$ , the MSE is less than  $10^{-3}$  based on 1000 Monte Carlo runs and we can always achieve perfect channel length estimation.
- **Channel estimation** Comparing with the result in [5], where we assume that perfect timing instance and the channel length, which are 17 and 8 separately in this example, are known, we can see that the performances are the same for  $SNR > 20\text{dB}$ . It is shown in Fig. 5.
- **SER for QPSK data symbols** The SER is obtained by simulation using: a)the joint blind timing and channel estimation algorithm provided in this paper; b)blind timing estimation and true channel; c)perfect knowledge of the timing instance and the channel. The results are shown in Fig. 6. When  $SNR > 20\text{dB}$ , all the three situations have SER less than  $10^{-5}$ .

## 5 Conclusion

In this paper, a receiver diversity based algorithm for joint blind timing synchronization and channel estimation is presented for the OFDM system. As far as SER is concerned, the proposed algorithm achieves

a performance close to the scheme that assumes exact knowledge of the transmission channel for high SNR scenarios.

## References

- [1] T. M. Schmidl and D. C. Cox, "Robust Frequency and Timing Synchronization for OFDM", *IEEE Transactions on Communications*, Vol. 45, No. 12, pp. 1613-21, December 1997.
- [2] H. Minn and V. K. Bhargava, "A Simple and Efficient Timing Offset Estimation for OFDM Systems", *Proc. Vehicular Tech. Conf.* Tokyo, Japan, pp. 51-55, March 2000.
- [3] E. G. Larsson, G. Liu, J. Li and G. B. Giannakis, "Joint Symbol Timing and Channel Estimation for OFDM Based WLANs", *IEEE Communication letters*, Vol. 5, No. 8, pp. 325-327, August 2001.
- [4] J. van de Beek, M. Sandell and P. O. Borjesson, "ML Estimation of Time and Frequency Offset in OFDM Systems", *IEEE Transactions on Signal Processing*, Vol. 45, No. 7, pp. 1800-05, July 1997.
- [5] H. Wang, Y. Lin and B. Chen, "Blind OFDM Channel Estimation Using Receiver Diversity", *Proc. 36th Annual Conference on Information Sciences and Systems*, Princeton, NJ, pp. 163-167, March 2002.
- [6] R. Van Nee and R. Prasad, "*OFDM for Wireless Multimedia Communications*", Artech House, 2000.
- [7] G.A.F. Seber and C.J. Wild, "*Nonlinear Regression*", John Wiley and Sons, 1988.

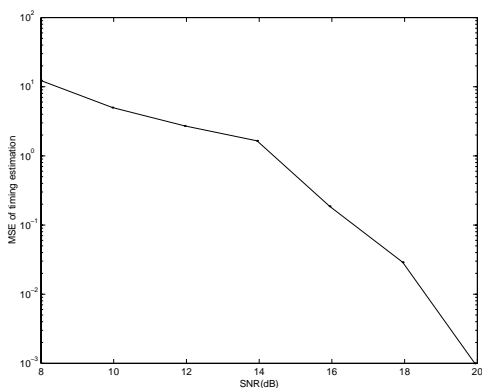


Figure 3: mean-squared error of timing estimation

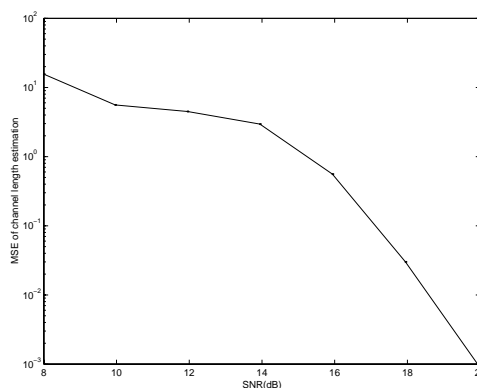


Figure 4: mean square error of channel length estimation

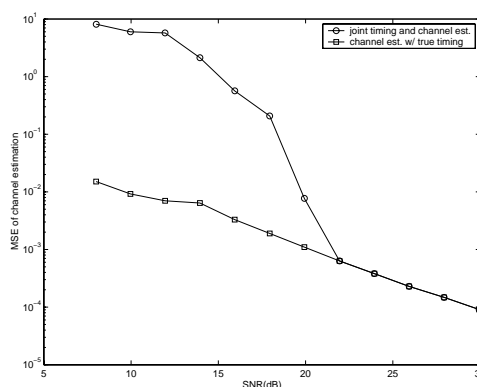


Figure 5: mean square error of channel estimation, for the first channel

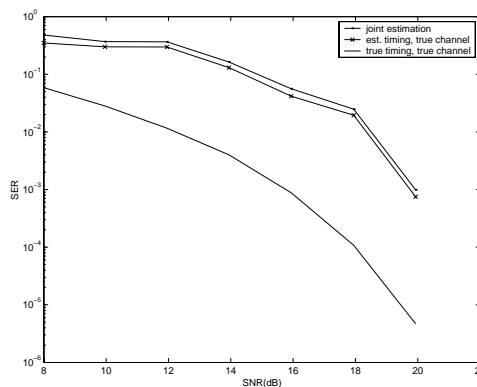


Figure 6: symbol error rate for 3 cases